ARTICLES

Journal of Semiconductors
(2022) 43, 082301
doi: 10.1088/1674-4926/43/8/082301

Research on quantum well intermixing of 680 nm AlGaInP/GaInP semiconductor lasers induced by composited Si–Si_3N_4 dielectric layer

Tianjiang He[1, 2], Suping Liu[1, †], Wei Li[1], Cong Xiong[1], Nan Lin[1, 2], Li Zhong[1, 2], and Xiaoyu Ma[1, 2]

[1]National Engineering Research Center for Optoelectronic Devices, Institute of Semiconductors, Chinese Academy of Sciences, Beijing 100083, China

[2]College of Materials Science and Optoelectronics, University of Chinese Academy of Sciences, Beijing 100049, China

Abstract: The optical catastrophic damage that usually occurs at the cavity surface of semiconductor lasers has become the main bottleneck affecting the improvement of laser output power and long-term reliability. To improve the output power of 680 nm AlGaInP/GaInP quantum well red semiconductor lasers, Si–Si_3N_4 composited dielectric layers are used to induce its quantum wells to be intermixed at the cavity surface to make a non-absorption window. Si with a thickness of 100 nm and Si_3N_4 with a thickness of 100 nm were grown on the surface of the epitaxial wafer by magnetron sputtering and PECVD as diffusion source and driving source, respectively. Compared with traditional Si impurity induced quantum well intermixing, this paper realizes the blue shift of 54.8 nm in the nonabsorbent window region at a lower annealing temperature of 600 °C and annealing time of 10 min. Under this annealing condition, the wavelength of the gain luminescence region basically does not shift to short wavelength, and the surface morphology of the whole epitaxial wafer remains fine after annealing. The application of this process condition can reduce the difficulty of production and save cost, which provides an effective method for upcoming fabrication.

Key words: high power semiconductor laser; rapid thermal annealing; composited dielectric layer; quantum well intermixing; optical catastrophic damage; nonabsorbent window

Citation: T J He, S P Liu, W Li, C Xiong, N Lin, L Zhong, and X Y Ma, Research on quantum well intermixing of 680 nm AlGaInP/GaInP semiconductor lasers induced by composited Si–Si_3N_4 dielectric layer[J]. *J. Semicond.*, 2022, 43(8), 082301. https://doi.org/10.1088/1674-4926/43/8/082301

1. Introduction

Lasers, optical fibers and semiconductor photonic devices are generally regarded as the three major inventions in the field of optics in the twentieth century. Among them, semiconductor lasers play an important role in the whole laser field because of their small volume, light weight and easy integration[1]. High power semiconductor lasers in the red band are widely used for pump sources, laser display, medical devices and laser lighting[2, 3]. However, the catastrophic optical damage (COD) that often occurs at the laser cavity surface is a major problem that hinders its power improvement and long-term service reliability[4–6]. This damage is due to the overload of laser power density and high cavity surface temperature, which causes the bandgap to shrink, and then promotes itself to absorb more photons, forming a positive feedback process, resulting in the melting and recrystallization of the cavity surface area[7].

Moreover, the device will fail in the range of tens of nanoseconds. An effective method to prevent this problem is to make a nonabsorbent window (NAW) at the laser cavity surface. As a post-treatment process, impurity induced quantum well hybrid technology has attracted extensive attention because of its advantages, such as easy process, low equipment requirements and low manufacturing cost. This research has been developed since it was found that the diffusion of Si impurities can promote the mutual diffusion of quantum barrier and quantum well components in the 1980s[8]. In 1985, Kaliski *et al.*[9] conducted Si impurity induced quantum well intermixing on AlGaAs/GaAs superlattices. At 750 °C annealing temperature and 144 h annealing time, the blue shift of the emission spectrum peak of quantum well is up to 85 nm. In 2010, Cong *et al.*[10] implanted InGaAs/AlAsSb double quantum well structure chip with Si ions, and obtained a blue shift of 160 nm under the condition of rapid thermal annealing (RTA) at 600 °C/1 min. There are only a few studies on Si impurity induced quantum well intermixing in China. In 2007, Peng[11] of Hebei University of technology conducted Si impurity diffusion and Si ion implantation on GaAs/AlGaAs semiconductor lasers to induce quantum well intermixing. However, the p-type dopant in the epitaxial layer is Zn, which hinders the diffusion of Si, resulting in a small blue shift. In 2020, Liu[12] performed secondary epitaxy of Si dielectric layer on the surface of InGaAs/AlGaAs quantum well semiconductor laser by means of MOCVD, and the devices displayed a distinct 52 nm blue shift under the condition of RTA 900 °C/180 s. A 93 nm blue shift was also obtained when annealed in tubular furnace at 825 °C/2 h, while the blue shift of the luminescence gain region under various experimental conditions after annealing

Correspondence to: S P Liu, spliu@semi.ac.cn
Received 10 FEBRUARY 2022; Revised 14 MARCH 2022.

can reach up to 65 nm. In regards to all of these doping methods, ion implantation[13, 14] methods appear to be inferior because of their high cost and they are incompetent because of their inevitable damage to the lattice, which will irreversibly do harm to the later device fabrications. In addition, when growing Si dielectric layer induced quantum well intermixing[15], the high temperature or long-time thermal annealing will not only damage the surface morphology of the epitaxial wafer[16] but will also cause the blue shift of the wavelength of the gain luminescence region[17]. Therefore, to solve these problems, the quantum well intermixing experiment is redesigned in this paper. The composited Si–Si_3N_4 dielectric layer is used to induce the quantum well intermixing of 680 nm semiconductor laser, through which the surface morphology of epitaxial wafer is not affected by thermal annealing at low temperature of 540–600 °C and at the same time the wavelength of the gain luminescence region basically does not change under the condition of ensuring a certain blue shift in the nonabsorbent window region. This approach will not only save the cost and improve the efficiency but will also effectively protect the sample, realizing a better intermixing affect.

2. Establishing a quantum well intermixing model

2.1. Component calculation

For 680 nm single quantum well GaInP/$Al_{0.53}$GaInP red semiconductor laser, Al, Ga and In atoms occupy group III lattice, while P atoms occupy group V lattice. Generally speaking, in III–V compound semiconductors, the two defects with the largest diffusion rate are group III vacancies V_{III} and group III interstitial atoms I_{III}. The mutual diffusion of Al and Ga atoms is mainly considered in the process of component calculation and simulation because In atoms are large and have a slow diffusion rate. In the process of component interdiffusion caused by impurity induction, it is mainly carried out in the form of Frenkel defect pairs through V_{III} and I_{III}[18]:

$$V_{Ga} \leftrightarrow V_{Ga} + (I_{Al} + V_{Al}) \leftrightarrow (V_{Ga} + I_{Al}) + V_{Al} \leftrightarrow V_{Al}, \quad (1)$$

$$I_{Ga} \leftrightarrow I_{Ga} + (V_{Al} + I_{Al}) \leftrightarrow (I_{Ga} + V_{Al}) + I_{Al} \leftrightarrow I_{Al}. \quad (2)$$

The initial concentration of Al component is:

$$C = \begin{cases} C_w, & |z| < d, \\ C_b, & |z| \geqslant d, \end{cases} \quad (3)$$

where C_w and C_b represent the component concentration of Al in the quantum well and quantum barrier, respectively. Taking the central position of the quantum well as the z-axis origin, the width of the quantum well is $2d$.

Setting the diffusion length to L_d and after the completion of quantum well mixing, the expression of Al component concentration in quantum well and quantum barrier is as follows[19]:

$$C(z) = C_1 + \frac{(C_2 - C_1)}{2}\left[\mathrm{erfc}\left(\frac{z+d}{2L_d}\right) + \mathrm{erfc}\left(\frac{-z+d}{2L_d}\right)\right]. \quad (4)$$

The width of the quantum well of the semiconductor laser epitaxial wafer used in this experiment is 7 nm, and the Al diffusion distance L_d is set to 0, 1, 2 and 3 nm. The Al component concentration can be calculated according to the diffusion distance after mixing, as shown in Fig. 1.

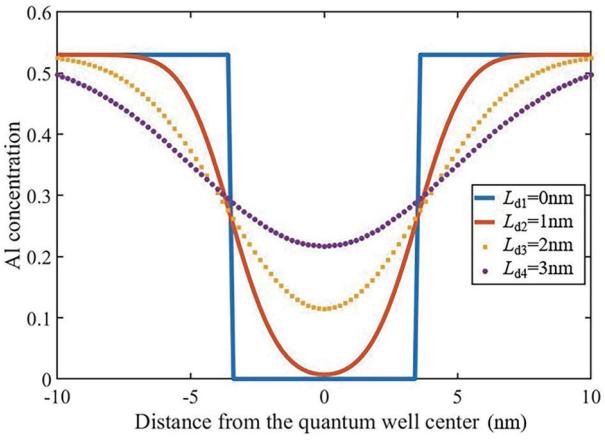

Fig. 1. (Color online) Variation of Al component concentration with diffusion distance.

From this figure it can be seen that when there is no diffusion, the content of Al in the well and barrier is 0 and 0.53, respectively. Meanwhile, the distribution of Al atoms in the well barrier shows an obvious step shape. When the diffusion length is short as L_d = 1 nm for example, Al occupies a relatively large portion in the well region so the quantum well region and quantum barrier region can maintain good heterojunction morphology. However, with the increase of diffusion length, when L_d = 2 nm, the Al component concentration in the well region gradually increases, and the Al component concentration at the interface between the well region and the barrier region gradually tends to be consistent. When the diffusion length L_d reaches 3 nm, the Al composition in the well and barrier tends to be the same, the obvious interface between the well region and the barrier region has not been observed, and the heterojunction state is difficult to maintain. This figure also shows that the quantum well mixing degree between the well region and the barrier region has been sufficient.

2.2. Blue shift simulation

According to the variation of Al component concentration with diffusion distance calculated in the previous section—that is, after the diffusion distances L_d are 0, 1, 2 and 3 nm—, the corresponding values of Al component concentrations in the quantum well are 0, 0.007, 0.115 and 0.217, respectively. The variation of quantum well gain spectrum with Al component concentration is simulated in this section, as shown in Fig. 2.

It can be seen that when the diffusion distance is small—that is, the Al component changes little—, the gain spectrum peak basically has no blue shift and the value of gain has a small variation. However, when the diffusion distance gradually increases, the gain spectrum peak blue shift also increases, while the gain value decreases. A 40 nm of blue shift is observed when the diffusion distance is 2 nm and the gain value is 88.5% of the original value.

2.3. Effect of temperature on component interdiffusion

In group III–V semiconductors, the point defect concentration is usually much less than the group III atom concentration (about 2×10^{22} cm^{-3}); that is, the mutual diffusion coeffi-

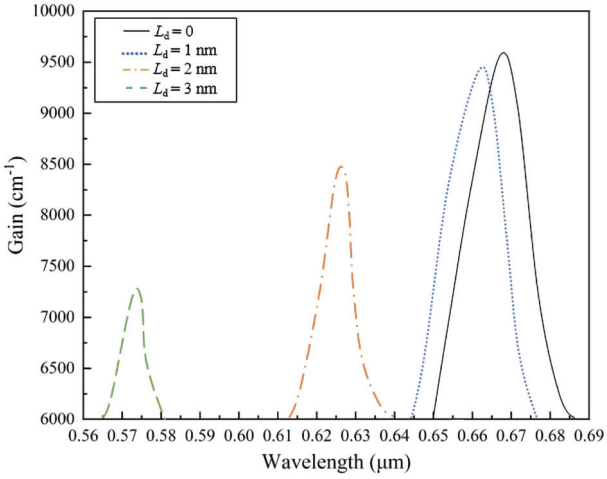

Fig. 2. (Color online) Variation of quantum well gain spectrum peaks with Al atom diffusion distances.

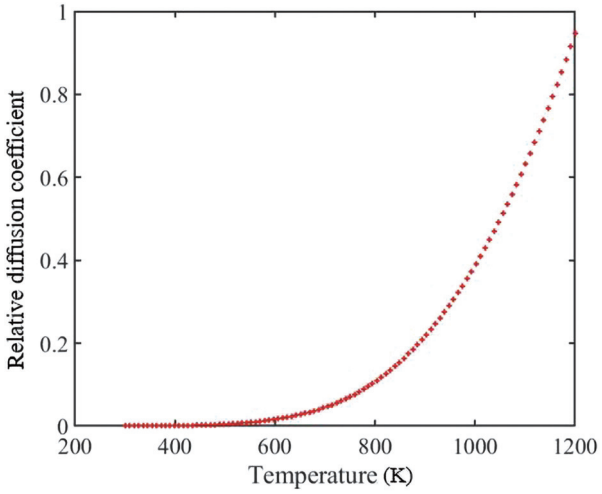

Fig. 3. (Color online) The relationship between the interdiffusion coefficient of group III atoms and temperature.

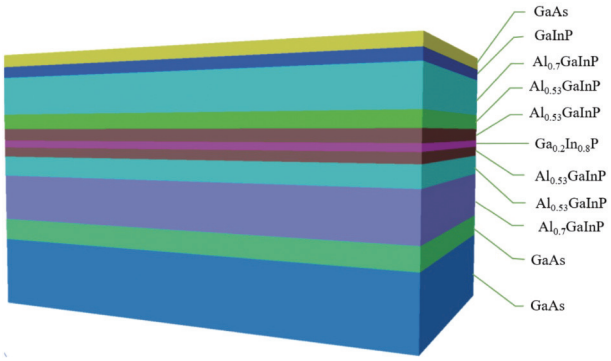

Fig. 4. (Color online) Schematic diagram of GaInP/AlGaInP QW semiconductor laser

cient is mainly determined by the point defect concentration. The mutual diffusion coefficient is expressed as[13]:

$$D_{\mathrm{III}} = f_1 D_{\mathrm{V_{III}}} [\mathrm{V_{III}}] + f_2 D_{\mathrm{I_{III}}} [\mathrm{I_{III}}], \tag{5}$$

where D_{III} is the mutual diffusion coefficient of group III atoms, f_1 and f_2 are constants containing information about crystal structure and group III lattice concentration.

Assuming that there are N lattice points in group III lattice and the vacancy occupation number is n, then the possible arrangement number is

$$G = \frac{N!}{n!\,(N-n)!}. \tag{6}$$

By using the Stirling formula, the Boltzmann entropy S can be written as:

$$\begin{aligned} S &= k_{\mathrm{B}} \ln G = k_{\mathrm{B}} \ln \frac{N!}{n!\,(N-n)!} \\ &= k_{\mathrm{B}} [NknN - n \ln n - (N-n) \ln (N-n)], \end{aligned} \tag{7}$$

and the free energy of the whole system can be expressed as:

$$F = E - TS = F_0 + nE_{\mathrm{V}} - k_{\mathrm{B}} T [NknN - n \ln n - (N-n) \ln (N-n)], \tag{8}$$

where E_{v} is the energy required to form a vacancy, F_0 is the partial free energy independent of the number of vacancies n, T is the temperature. In this system, the equilibrium is determined by minimizing the free energy and by taking the derivative of F to n we get

$$\frac{\partial F}{\partial n} = E_{\mathrm{V}} + k_{\mathrm{B}} T \ln \frac{n}{N-n} = 0, \tag{9}$$

$$\frac{n}{N-n} = \exp\left(-\frac{E_V}{k_{\mathrm{B}} T}\right). \tag{10}$$

In this formula, the number of lattice points N is greater than vacancies n in the crystal. This can be simplified as:

$$n = N \exp\left(-\frac{E_{\mathrm{V}}}{k_{\mathrm{B}} T}\right). \tag{11}$$

Then, the normalized thermal equilibrium concentrations of group III vacancy and group III interstitial atoms are:

$$[V_{\mathrm{III}}] = \exp(-E_{\mathrm{V}}/k_{\mathrm{B}} T), \tag{12}$$

$$[I_{\mathrm{III}}] = \exp(-E_I/k_{\mathrm{B}} T). \tag{13}$$

By introducing these two formulas, the expression of the mutual diffusion coefficient of group III atoms with temperature can be obtained:

$$D_{\mathrm{III}} = f_1 D_{\mathrm{V_{III}}} \exp(-E_{\mathrm{V}}/k_{\mathrm{B}} T) + f2 D_{\mathrm{I_{III}}} \exp(-E_I/k_{\mathrm{B}} T). \tag{14}$$

From the Fig. 3, it can be seen that the value of the relative diffusion coefficient D increases gradually with the increase of temperature. It is proven that the two coefficients are close to the exponential relationship. When the temperature is higher than 800 K, the value of relative diffusion coefficient D increases sharply. This figure also shows that high temperature annealing is a necessary process in quantum well intermixing technology[20].

3. Experimental process and analysis

3.1. Epitaxial structure

The 680 nm quantum well semiconductor laser used in this experiment was prepared on n-GaAs substrate by aix-200/4 system low-voltage MOCVD equipment. As shown in Fig. 4, from the bottom to top, the structure of the epitaxial

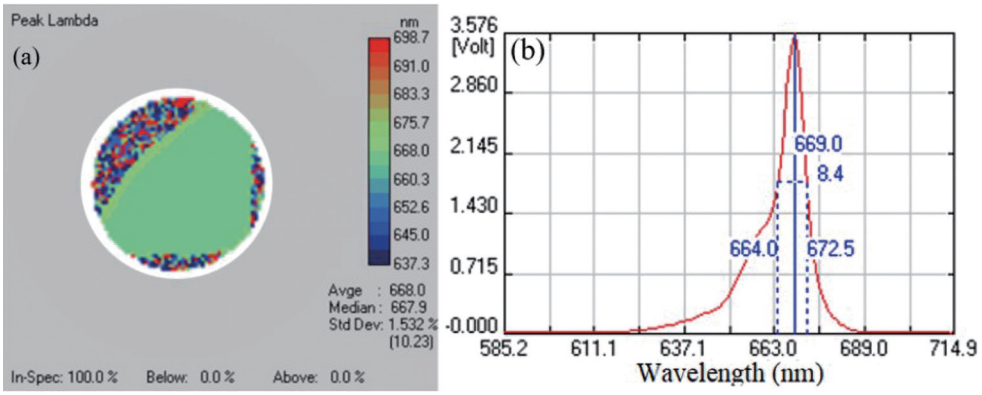

Fig. 5. (Color online) PL spectrum of GaInP/AlGaInP quantum well laser. (a) The mapping results of PL testing. (b) PL spectrum of epitaxial layer.

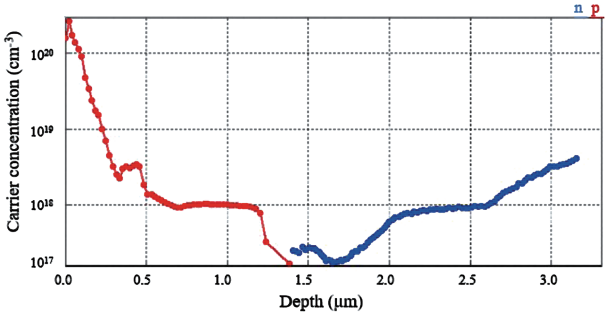

Fig. 6. (Color online) ECV test results of GaInP/AlGaInP quantum well epitaxial layer.

wafer is: 200 nm GaAs buffer layer, 2000 nm $Al_{0.7}GaInP$ confinement layer, 120 nm $Al_{0.53}GaInP$ waveguide layer, 20 nm $Al_{0.53}GaInP$ barrier, 7 nm $Ga_{0.2}In_{0.8}P$ QW layer, 20 nm $Al_{0.53}GaInP$ barrier layer, 120 nm $Al_{0.53}GaInP$ waveguide layer, 1800 nm $Al_{0.7}GaInP$ confinement layer, 100 nm GaInP cladding layer and 150 nm GaAs contact layer.

Before manufacturing the experiment, it is essential to test the PL spectrum and Electrochemical Cyclic Voltammetry (ECV) of the epitaxial wafer, which shows the key information of light intensity, peak wavelength and carrier concentration, and carrier distribution. The test results are shown in Figs. 5 and 6, in which the peak value of PL spectrum is 669 nm and the luminous intensity of the sample is relatively uniform. It can also be seen from the ECV test that the quality of the epitaxial wafer meets our expectations.

3.2. Effect of a single dielectric layer on quantum well intermixing

The lift-off technique process is adopted, as shown in Fig. 7.

The specific operation process is as follows. First, photolithography is carried out on the epitaxial wafer to form a gain luminescence region and nonabsorbent window region. Then, we sputter a layer of Si with sputtering equipment under the conditions of sputtering pressure of 1.3 Pa, sputtering power of 100 W, argon flow rate of 50 sccm and sputtering time of 30 min. By using the ellipsometry, the thickness and refractive index of Si dielectric layer were 100.85 nm and 3.4607, respectively. A whole epitaxial wafer was cut into 6 × 6 mm^2 pieces followed by using rtp-500 rapid annealing furnace to handle these pieces. The annealing temperature was set to 540, 560 and 580 °C, while the annealing temperature remained unchanged for 10 min. After annealing, we remove the Si dielectric layer with KOH solution and observe the sample surface under the condition of annealing at 580 °C/10 min with a metallographic microscope, as shown in Fig. 8.

From this figure it can be seen that the surface quality of the sample remained fine after annealing, while the PL spectra peak of Si covered region and non Si covered region were both 668.9 nm at these three temperatures. Taking the error of measurement into consideration, it can be considered that there is no blue shift. Fig. 9 shows the PL spectrum under the annealing condition of 580 °C/10 min.

It can be concluded that under this temperature range, quantum well intermixing could not happen if the condition is only simply thermal annealing[21] or growth of a single Si dielectric layer.

3.3. Effect of composited dielectric layers on quantum well intermixing

First prepare the same epitaxial wafer and then use PECVD equipment to grow 100 nm Si_3N_4 after completing the process described in Section 3.2, as shown in Fig. 10.

Similarly, a wafer is cut into 6 × 6 mm^2 small standard pieces, which were consequently annealed under the condition of 540–600 °C/10 min with the temperature gradient of 20 °C. We found that there was basically no blue shift in the Si_3N_4 covered region, while the PL spectrum of Si–Si_3N_4 covered region is shown in Fig. 11.

It can be observed from this figure that with the gradual increase of annealing temperature, the wave peak of the spectrum gradually blue shifted. At 540 °C, the blue shift was 24 nm, while at 600 °C the blue shift reached 54.8 nm and the luminous intensity of all samples maintained more than 75% of the origin sample. This indicates that nonabsorbent window regions and gain luminescence regions were well realized.

An ECV test was carried out on the sample that was annealed at 580 °C/10 min, the result is shown in Fig. 12.

Compared with the ECV test result of the original sample, near 1.3 μm, the p-type doping concentration decreased while the n-type doping concentration increased. This indicates that Si impurities diffused into the sample and became n-type donors[22].

3.4. Effect of cyclic annealing

To avoid damage caused to the quantum well epitaxial wafer caused by long annealing time or high annealing temperature, we conducted three periods of annealing and the

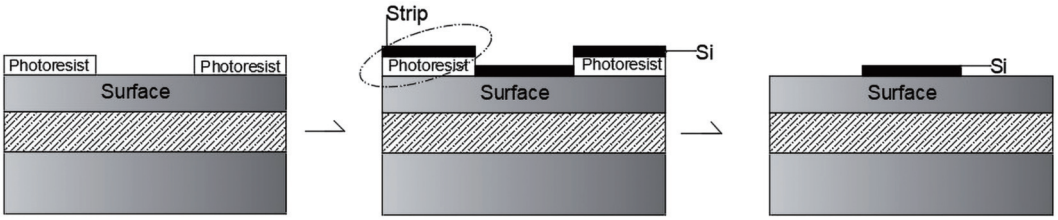

Fig. 7. The process of lift-off technique.

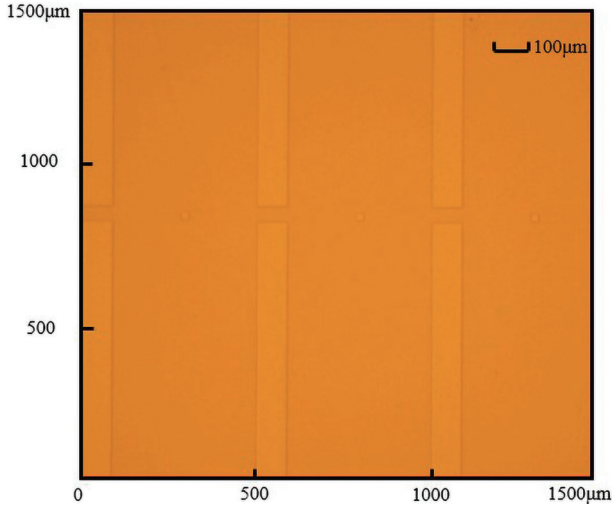

Fig. 8. (Color online) Sample surface after annealing at 580 °C/10 min.

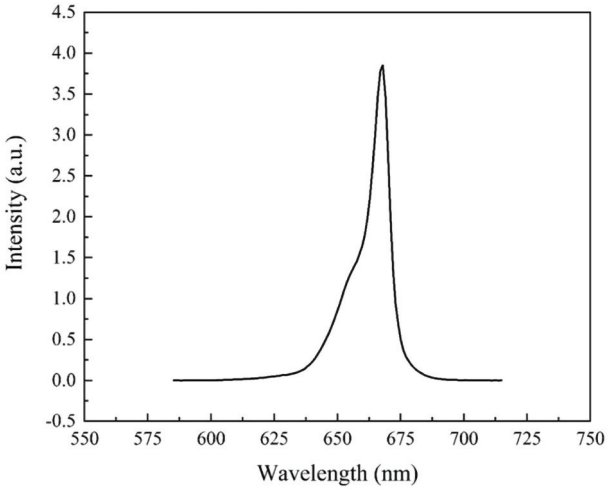

Fig. 9. The PL spectrum under the annealing condition of 580 °C/10 min.

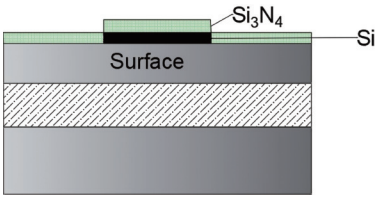

Fig. 10. (Color online) Schematic diagram after growing Si–Si_3N_4 composited dielectric layers.

temperature of each period was 580 °C and the annealing time was 10 min. After one annealing period was completed and the temperature was cooled to room temperature, we repeated the same experiment three times. We then tested the PL spectrum for each time, as shown in Fig. 13.

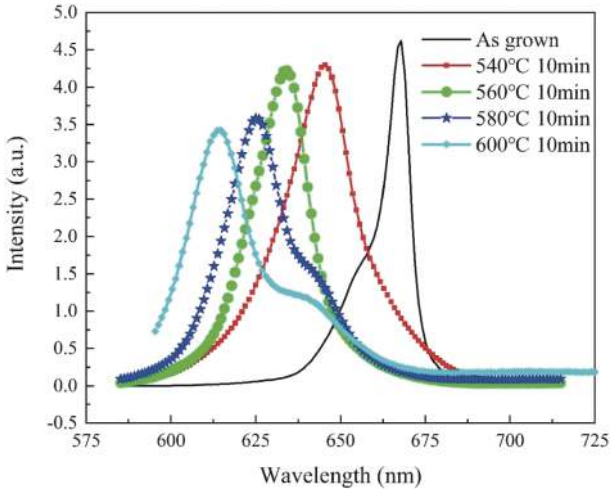

Fig. 11. (Color online) The PL spectra at different annealing temperatures.

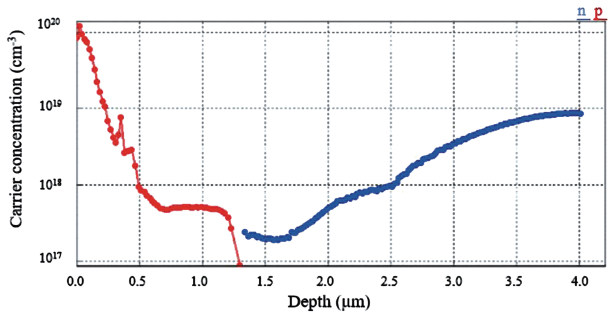

Fig. 12. (Color online) ECV test result of the sample annealed at 580 °C/10 min.

It can be found from this figure that the luminescence intensity did not decrease significantly with the increase of cyclic annealing times, and the blue shifts were 42.9, 45.7 and 48 nm respectively from one to three annealing times. This demonstrates that under the condition of 580 °C/10 min cyclic annealing, even if it can promote the increase of blue shift, the increase was limited.

3.5. Stress between dielectric layers

A thin film stress tester was used to test the stress between dielectric layers, as shown in Table 1.

The stress of 100 nm Si_3N_4 on GaAs substrate is –1204.315 MPa and the stress on Si substrate is –755.056 MPa, which is also relatively large. The surface compressive stress of GaAs will contribute to the generation of more Ga vacancy defects[23], and then produce a stronger quantum well intermixing effect. Therefore, it is speculated that the stress applied by Si_3N_4 made Si impurities diffuse into the epitaxial wafer during annealing, promoting the mutual diffusion of quantum well and quantum barrier components. Meanwhile,

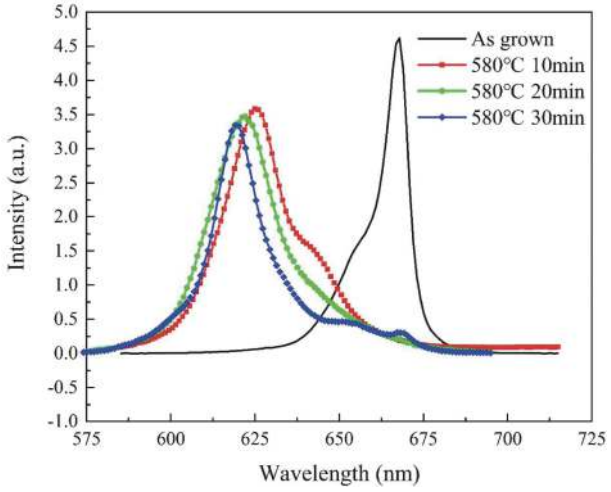

Fig. 13. (Color online) The PL spectra of the samples after annealing different cycles.

Table 1. Stress between dielectric layers.

Substrate	Dielectric layer	Stress (MPa)
GaAs	100 nm Si_3N_4	–1204.315
GaAs	100 nm Si	–570.124
Si	100 nm Si_3N_4	–755.056

the single Si dielectric layer is difficult to diffuse into the epitaxial wafer due to its small diffusion coefficient in GaAs.

4. Conclusion

In this paper, we propose the use of Si–Si_3N_4 composited dielectric layers to induce quantum well intermixing of 680 nm red semiconductor lasers. Under the condition of low annealing temperature of 540–600 °C and annealing time of 10 min, the blue shift difference between nonabsorbent window region and gain luminescence region greater than 30 nm is well realized and the luminous intensities are also maintained at more than 75% of the original sample. Moreover, in this temperature range, only simple thermal annealing or growth of single Si dielectric layer will not cause quantum well intermixing, while the large stress exerted by Si_3N_4 will promote the diffusion of Si in GaAs during thermal annealing and induce quantum well intermixing. This method will not only ensure the good lattice quality of the epitaxial wafer surface but will also reduce the process difficulty, which is conducive to the later device fabrication and provides an effective scheme to improve the COD threshold of 680 nm band semiconductor lasers.

Acknowledgements

This work was supported by the National Natural Science Foundation of China (NNSFC) (Grant No.62174154).

References

[1] Hu Y, Liang D, Mukherjee K, et al. III/V-on-Si MQW lasers by using a novel photonic integration method of regrowth on a bonding template. Light Sci Appl, 2019, 8(1), 93

[2] Lu H Y, Tian S C, Tong C Z, et al. Extracting more light for vertical emission: high power continuous wave operation of 1.3-μm quantum-dot photonic-crystal surface-emitting laser based on a flat band. Light Sci Appl, 2019, 8(6), 944

[3] Yuan Q H, Jing H Q, Zhang Q Y, et al. Development and applications of GaAs-based near-infrared high power semiconductor lasers. Laser Optoelectron Prog, 2019, 56(4), 040003

[4] Sin Y, Ives N, LaLumondiere S, et al. Catastrophic optical bulk damage (COBD) in high power multi-mode InGaAs-AlGaAs strained quantum well lasers. High-Power Diode Laser Technology and Applications IX, 2011, 791803

[5] Tian W N, Xiong C, Wang X, et al. Impurity-free vacancy diffusion induces intermixing in GaInP/AlGaInP quantum wells using GaAs encapsulation. Chin J Lumin, 2018, 39(8), 5

[6] Chinone N, Nakashima H, Ito R. Long-term degradation of GaAs-$Ga_{1-x}Al_xAs$ DH lasers due to facet erosion. J Appl Phys, 1977, 48(3), 1160

[7] He T J, Jing H Q, Zhu L N, et al. Research on quantum well intermixing of 915 nm InGaAsP/GaAsP primary epitaxial wafers. Acta Opt Sinica, 2022, 42(1), 0114003

[8] Deppe D G, Holonyak N. Atom diffusion and impurity-induced layer disordering in quantum well III-V semiconductor heterostructures. J Appl Phys, 1988, 64(12), R93

[9] Kaliski R W, Ito C R, McIntyre D G, et al. Influence of annealing and substrate orientation on metalorganic chemical vapor deposition GaAs on silicon heteroepitaxy. J Appl Phys, 1988, 64(3), 1196

[10] Cong G W, Akimoto R, Gozu S, et al. Simultaneous generation of intersubband absorption and quantum well intermixing through silicon ion implantation in undoped InGaAs/AlAsSb coupled double quantum wells. Appl Phys Lett, 2010, 96(10), 221115

[11] Peng H T. Improving the COD level of high-power semiconductor lasers using quantum well intermixing. Tianjin: Hebei University of Technology, 2007

[12] Liu C C, Lin N, Xiong C, et al. Intermixing in InGaAs/AlGaAs quamtum well structures induced by the interdiffusion of Si impurities. Chin Opt, 2020, 13(1), 203

[13] Zhou J T, Zhu H L, Cheng Y B, et al. Low energy helium ion implantation induced quantum-well intermixing. J Semicond, 2007, 28(1), 47

[14] Ge X H, Zhang R Y, Guo C Y, et al. Stduy of multiple factors ion-implantation-induced quantum wells intermixing. Laser Optoelectron Prog, 2020, 57(1), 7

[15] Fang X H, Bao X M. Study on mechanism of Si diffusion in GaAs. J Semicond, 1996(17), 922

[16] Ali N B, Harrison I, Ho H P, et al. Annealing-induced dislocation loops in Si-doped GaAs-AlAs superlattices. J Mater Sci - Mater Electron, 1993, 4(1), 29

[17] Yamada N, Roos G, Harris J S. Threshold reduction in strained InGaAs single quantum well lasers by rapid thermal annealing. Appl Phys Lett, 1991, 59(9), 1040

[18] Zhou L. Research on anti catastrophic optical damage of high power semiconductor laser diodes. Changchun: Changchun University of Science and Technology, 2014

[19] Wang X, Zhao Y H, Zhu L N, et al. Impurity-free vacancy diffusion induces quantum well intermixing in 915 nm semiconductor laser based on SiO_2 film. Acta Photonica Sinica, 2018, 47(3), 7

[20] Lin S J, Li J J, He L J, et al. Enhanced AlGaAs/InGaAs quantum well intermixing by the technology of cycles annealing. J Optoelectron Laser, 2014, 25(8), 5

[21] Lin T, Ning S H, Li J J, et al. Temperature-dependent photoluminescence characteristics of strained GaInP quantum well structure. Acta Photonica Sinica, 2019, 48(1), 6

[22] Tjeertes D, Vela A, Verstijnen T, et al. Atomic-scale study of Si-doped AlAs by cross-sectional scanning tunneling microscopy and density functional theory. Phys Rev B, 2021, 104(12), 125433

[23] Liu C C, Lin N, Ma X Y, et al. High performance InGaAs/AlGaAs quantum well semiconductor laser diode with non-absorption window. Chin J Lumin, 2022, 43(1), 9

Tianjiang He got his BS from Huazhong University of Science and Technology in 2019. Now he is a PhD student at University of Chinese Academy of Sciences under the supervision of Prof. Xiaoyu Ma. His research focuses on high power semiconductor lasers.

Suping Liu got her BS degree in 1992 and MS degree in 1995 at Jilin University. Then she joined Xiaoyu Ma Group at Institute of Semiconductors, Chinese Academy of Sciences as a senior engineer. Her research interests include high power semiconductor lasers and their components, solid state lasers and storage lasers.